ELSEVIER

Journal of Fluids and Structures 20 (2005) 719–733

JOURNAL OF FLUIDS AND STRUCTURES

www.elsevier.com/locate/jfs

Hydroelasticity of a circular plate on water of finite or infinite depth

A.I. Andrianov*, A.J. Hermans

Department of Applied Mathematics, Faculty of Electrical Engineering, Mathematics and Computer Science, Delft University of Technology, Mekelweg 4, 2628 CD Delft, The Netherlands

Received 23 September 2003; accepted 4 March 2005
Available online 23 May 2005

Abstract

This paper considers the diffraction of incident surface waves by a floating elastic circular plate. We investigate the hydroelastic response of the plate to a plane incident wave for two cases of water depth. An analytic and numerical study is presented. An integro-differential equation is derived for the problem and an algorithm of its numerical solution is proposed. The representation of the solution as series of Bessel functions is the key idea of the approach. After a brief introduction and formulation of the problem, we derive the main integro-differential equation by the use of the thin plate theory and Green's theorem. The plate deflection, the free-surface elevation and the Green's function are expressed in cylindrical coordinates as series of Bessel functions. For the coefficients, a set of algebraic equations is obtained, yielding the approximate solution for the case of infinite water depth. Then a solution is obtained for the general case of finite water depth analogously. The exact solution is approximated by taking a finite number of roots of the dispersion relation into account. Numerical results for the plate deflection, initiated wave pattern and free-surface elevation are presented for various physical parameters of the problem, together with some remarks on the computation and discussion.

Keywords: Circular plate; Diffraction; Hydroelastic analysis; Integro-differential equation; plate-water interaction

1. Introduction

The hydroelastic analysis of a very large floating platform (VLFP) in water waves received a great deal of attention because of the design of large floating offshore structures for airports or runaways, breakwaters, artificial islands, industrial space, etc. The objective of the study is to investigate the behavior of a VLFP and its influence on the surface waves, i.e., diffraction of the waves by the VLFP. The main idea in the proposed concepts is to build a very large mat-like structure; therefore, the thickness of VLFP is very small in comparison to its horizontal parameters. This kind of floating platform can be modelled as a flexible thin plate with elastic properties. This theory can also be used to describe the interaction between large ice fields and surface waves by inserting the ice physical properties instead of the plate parameters. As water depth plays an important role in this kind of problem, the theory is divided into three cases: very deep water (depth is considered to be infinite), water of finite depth, and shallow water.

*Corresponding author. Tel.: +31 15 2783613; fax: +31 15 2787295.
E-mail addresses: a.i.andrianov@ewi.tudelft.nl (A.I. Andrianov), a.j.hermans@ewi.tudelft.nl (A.J. Hermans).
URL: http://www.andrianov.org, http://ta.twi.tudelft.nl/mf/users/hermans.

0889-9746/$ - see front matter
doi:10.1016/j.jfluidstructs.2005.03.002

Recently, a number of papers were published considering the hydroelastic analysis of VLFP. A very detailed literature survey for this problem has been published recently by Watanabe et al. (2004). There are several approaches used to describe the interaction between VLFPs and surface waves. We can distinguish the following: asymptotic theory for short waves, e.g., Ohkusu and Namba (1996); parabolic approximation, e.g., Takagi (2002); ray theory (Hermans, 2003); variational equation method (Meylan, 2001); eigenfunction expansion method with determination of the eigenfunctions numerically; Wiener-Hopf technique; Galerkin method, etc. Many of these results have been presented at the International Workshops on Water Waves and Floating Bodies.

The analytical solution for the plates having one or two infinite dimensions, which simplify significantly the complexity of analysis, can be derived with use of any of the approaches given above. For the plates of finite extent numerical methods are often used. Mainly the indicated articles studied the plates of rectangular planform, while there are only few papers considering arbitrarily shaped VLFPs. Several papers, studying circular plates, were presented recently at international conferences. For the circular ice floe, the problem was solved by Meylan and Squire (1996) for the case of deep water by use of the eigenfunction method. A closed-form solution for buoyant circular plate floating on shallow water was developed by Zilman and Miloh (2000) with use of Stoker's shallow water theory. This problem was also solved by Tsubogo (2001) by an advanced boundary element method. The plate floating on shallow water under an external load has been considered by Sturova (2003). For a finite water depth the problem was solved by Watanabe et al. (2003) with use of the Galerkin method and Mindlin plate theory. Peter et al. (2003) presented a solution for the same problem based on decomposing the solution into angular eigenfunctions. The present authors solved the problem of hydroelastic response of a circular plate for water of finite and infinite depth; some preliminary results were presented in Andrianov and Hermans (2004).

Here we consider the problem for a plate in the form of the circular disk for two different cases: deep water and water of finite depth. An analytical study is presented for both cases. The circular plate floats at the surface of an ideal fluid. We consider the circular plate with constant flexural rigidity and homogeneous stiffness. The edge of the plate is free of shear forces, bending and twisting moments. We use Green's theorem and an integro-differential formulation for the deflection, as derived and described in Hermans (2003) and Andrianov and Hermans (2003). The plate deflection, generated by incoming surface waves is represented as a series of Bessel functions, multiplied by cosine functions. The approach presented allows us to study the plate deflection, the initiated wave pattern generated by the plate motion, and the free-surface elevation.

At first, we study the behavior of the circular plate floating on the surface of the water of infinite depth. This would appear to be a rather theoretical problem, but it is a good starting point to find a solution for the general and most important case of finite water depth. Next, we consider the finite water depth case, where the general analysis and set of equations are more complicated, as more roots of the water dispersion relation have to be taken into account. The numerical results obtained are presented and discussed for various physical parameters of the problem. The conclusions and the summary for possible extensions of the approach are given in the last section.

2. Formulation of the problem

In this section we derive the general mathematical formulation for the problem under consideration. The floating thin elastic circular plate of radius r_0 covers a part of the surface of the water, which is assumed to be an ideal incompressible fluid. The value of water depth h is infinite for the case of deep water and finite and constant for the other case. We assume that no space exists between the free-surface and the plate. The flexural rigidity of circular plate is constant.

The plate deflection is generated by incoming surface waves. We assume that waves propagate in otherwise still water. Also, it is assumed that incoming waves are propagating in the positive x-direction without loss of generality. The wave amplitude is assumed to be small in comparison with other parameters of the problem.

The problem is considered in polar coordinates; they are related to Cartesian coordinates by $\rho^2 = x^2 + y^2$, $\varphi = \arctan y/x$. The geometric sketch of the plate is shown in Fig. 1. At the free-surface $z = 0$, we denote the plate region as $\mathscr{P}$ ($\rho \leqslant r_0$; $\varphi = [0, 2\pi]$) with the plate contour $\mathscr{S}$ ($\rho = r_0$; $\varphi = [0, 2\pi]$) and the open fluid region as $\mathscr{F}$ ($\rho > r_0$; $\varphi = [0, 2\pi]$).

The velocity potential is introduced by $\nabla_{(3)}\Phi(\rho, \varphi, z, t) = \mathbf{V}(\rho, \varphi, z, t)$, where $\mathbf{V}(\boldsymbol{\rho}, t)$ is the fluid velocity vector. The Laplacian in cylindrical coordinates is defined as

$$\nabla^2_{(3)} = \Delta_{(3)} = \frac{\partial^2}{\partial\rho^2} + \frac{1}{\rho}\frac{\partial}{\partial\rho} + \frac{1}{\rho^2}\frac{\partial^2}{\partial\varphi^2} + \frac{\partial^2}{\partial z^2},$$

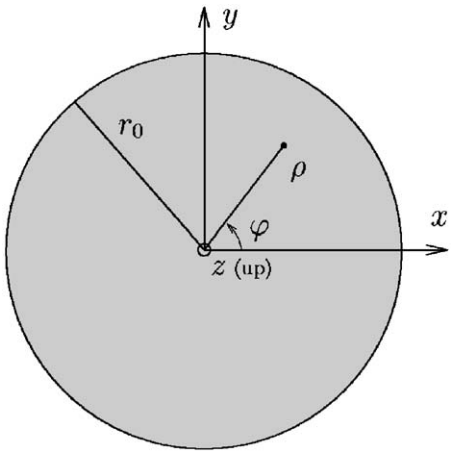

Fig. 1. The geometry and coordinate system of the problem.

where the subscript (3) is used for three-dimensional operators, to distinguish them from two-dimensional operators Δ and ∇ at the free surface. The velocity potential $\Phi(\boldsymbol{\rho}, t)$ is a solution of the governing Laplace equation in the fluid, $z<0$,

$$\Delta_{(3)}\Phi = 0, \tag{1}$$

together with the boundary conditions at the free surface and at the bottom. The linearized kinematic condition in the plate and water regions, $z = 0$, has the form

$$\frac{\partial \Phi}{\partial z} = \frac{\partial w}{\partial t}, \tag{2}$$

where $w(\rho, \varphi, t)$ denotes either the deflection of the plate in $\mathscr{P}$, or the free-surface elevation in $\mathscr{F}$, and t is the time. The linearized dynamic condition, derived from the linearized Bernoulli equation, is written as

$$\frac{P - P_{\text{atm}}}{\rho_w} = -\frac{\partial \Phi}{\partial t} - gw, \tag{3}$$

at $z = 0$, where ρ_w is the density of the water, g is gravitational acceleration, $P(\rho, \varphi, t)$ is the pressure in the fluid, and P_{atm} is the atmospheric pressure. Relations (2) and (3) are kinematic and dynamic conditions at the free surface, and the linearized free-surface condition in the open water region $\mathscr{F}$, $z = 0$, takes the form

$$\frac{\partial \Phi}{\partial z} = -\frac{1}{g}\frac{\partial^2 \Phi}{\partial t^2}. \tag{4}$$

In the finite water-depth case the normal potential equals zero at the bottom $z = -h$

$$\frac{\partial \Phi}{\partial z} = 0. \tag{5}$$

The platform is modelled as an elastic plate with zero thickness. Such a model can be applied, as described above, due to the small thickness and shallow draft of the platform. To describe the deflection of the plate $w(\rho, \varphi)$, we apply the isotropic thin plate theory, see, e.g., Timoshenko et al. (1974), which leads to a differential equation at $z = 0$ in the plate area $\mathscr{P}$, known as the Gehring–Kirchhoff equation of plate motion

$$D\Delta^2 w + m\frac{\partial^2 w}{\partial t^2} = P - P_{\text{atm}}, \tag{6}$$

where m is the mass of unit area of the platform, D is the flexural rigidity, expressed in terms of Young's modulus E, Poisson's ratio ν and the plate thickness h_p as follows:

$$D = \frac{Eh_p^3}{12(1-\nu^2)}.$$

From now on, the Laplacian is a two-dimensional operator

$$\nabla^2 = \Delta = \frac{\partial^2}{\partial\rho^2} + \frac{1}{\rho}\frac{\partial}{\partial\rho} + \frac{1}{\rho^2}\frac{\partial^2}{\partial\varphi^2}.$$

Following the procedure described in Hermans (2003) and Andrianov and Hermans (2003), we apply the operator $\partial/\partial t$ to (6) and use the surface conditions (2) and (3) to arrive at the following differential equation for the potential Φ acting on the plate at $z = 0$:

$$\left\{\frac{D}{\rho_w g}\Delta^2 + \frac{m}{\rho_w g}\frac{\partial^2}{\partial t^2} + 1\right\}\frac{\partial\Phi}{\partial z} + \frac{1}{g}\frac{\partial^2\Phi}{\partial t^2} = 0. \tag{7}$$

We consider harmonic waves and their potential can be written in the form

$$\Phi(\rho, \varphi, z, t) = \phi(\rho, \varphi, z)\mathrm{e}^{-\mathrm{i}\omega t}, \tag{8}$$

where ω is the wave frequency. In the same way, the deflection is written as $w(\rho, \varphi, t) = w(\rho, \varphi)\mathrm{e}^{-\mathrm{i}\omega t}$. Then we reduce time-dependence and consider waves of a single frequency ω and obtain at $z = 0$ for the plate region $\mathscr{P}$

$$\{\mathscr{D}\Delta^2 - \mu + 1\}\frac{\partial\phi}{\partial z} - K\phi = 0, \tag{9}$$

where we have introduced $K = \omega^2/g$ and the structural parameters $\mathscr{D} = D/\rho_w g$, $\mu = m\omega^2/\rho_w g$, which are constant. For the open water region $\mathscr{F}$, we have

$$\frac{\partial\phi}{\partial z} - K\phi = 0. \tag{10}$$

All definitions, given above, are valid for both infinite and finite water-depth cases.

The potential of the incident wave for water of finite depth has the form

$$\phi^{\mathrm{inc}}(\rho, \varphi, z) = \frac{\cosh k_0(z + h)}{\cosh k_0 h}\frac{gA}{\mathrm{i}\omega}\,\mathrm{e}^{\mathrm{i}k_0\rho\,\cos\,\varphi}, \tag{11}$$

where k_0 is the wavenumber, and A is the wave amplitude of the incident wave. The wavenumber k_0 is the positive real solution of the water dispersion relation

$$k\,\tanh\,kh = K. \tag{12}$$

For deep water, the potential is represented in the form

$$\phi^{\mathrm{inc}}(\rho, \varphi, z) = \frac{gA}{\mathrm{i}\omega}\,\mathrm{e}^{\mathrm{i}k_0\rho\,\cos\,\varphi + k_0 z}. \tag{13}$$

In this case the wavenumber is $k_0 = K = \omega^2/g$.

The wavelength of incoming waves is $\lambda = 2\pi/k_0$. In a practical situation, the radius of the floating circular plate r_0 might be of the order of a thousand meters, while the wavelength λ is of the order of a hundred meters. Therefore, we consider and compute numerically the situation when the wavelength is less than the diameter of the plate ($\lambda < 2r_0$), but our approach is also valid for the case of small circular disks ($\lambda > 2r_0$).

The edge of the circular plate is free of vertical shear forces, bending and twisting moments. Hence, the free edge conditions at the plate contour $\mathscr{S}$ are written as

$$\left\{\nabla^2 - \frac{(1 - \nu)}{\rho}\left(\frac{\partial}{\partial\rho} + \frac{1}{\rho}\frac{\partial^2}{\partial\varphi^2}\right)\right\}w = 0, \tag{14}$$

$$\left\{\frac{\partial}{\partial\rho}\nabla^2 + \frac{(1 - \nu)}{\rho^2}\left(\frac{\partial}{\partial\rho} - \frac{1}{\rho}\right)\frac{\partial^2}{\partial\varphi^2}\right\}w = 0. \tag{15}$$

3. Green's function and deflection

The main objective of our study is to determine the plate deflection by solving a set of equations at the plate $\mathscr{P}$. An integro-differential equation can be derived if we apply the Green's theorem. To complete the system, we use the free edge conditions. In this section we describe the Green's and deflection functions and the operations on the

corresponding Bessel functions for the circular plate. The expressions for the Green's function for water of infinite and finite depth can be found in Wehausen and Laitone (1960).

We introduce the Green's function for a source within the fluid, that in Cartesian coordinates satisfies $\Delta_{(3)}\mathscr{G} = 4\pi\delta(\mathbf{x}-\boldsymbol{\xi})$, where δ is the Dirac δ-function, $\mathbf{x}$ is a source point and $\boldsymbol{\xi}$ is an observation point. The Green's function obeys the boundary conditions at the free surface ($\mathscr{G}_z = K\mathscr{G}$), and at the bottom, and the radiation condition.

For deep water, the three-dimensional Green's function can be written in the following form:

$$\mathscr{G}(\mathbf{x},\boldsymbol{\xi}) = -\frac{1}{\varrho}+\frac{1}{\varrho_1}-2\int_{\mathscr{L}}\frac{k}{k-k_0}\,\mathrm{J}_0(kR)\mathrm{e}^{k(z+\zeta)}\,\mathrm{d}k, \tag{16}$$

where $\varrho^2 = R^2+(z-\zeta)^2$, $\varrho_1^2 = R^2+(z+\zeta)^2$, R is the horizontal distance, and $\mathrm{J}_0(kR)$ is the Bessel function. The contour of integration $\mathscr{L}$ is shown in Fig. 2. It passes underneath the singularity $k = k_0$ to fulfil the radiation condition.

The Green's function in polar coordinates $\mathscr{G}(\rho,\varphi,z;r,\theta,\zeta)$ for the source and observation points at $z=\zeta=0$ is written as

$$\mathscr{G}(\rho,\varphi;r,\theta) = -2\int_{\mathscr{L}}\frac{k}{k-k_0}\,\mathrm{J}_0(kR)\,\mathrm{d}k, \tag{17}$$

where the horizontal distance R in polar coordinates is $R^2(\rho,\varphi;r,\theta) = \rho^2+r^2-2\rho r\cos(\theta-\varphi)$. Here ρ and r are the distances from the center of the plate to the source and observation points, respectively, and $\theta-\varphi$ is the angle between r and ρ.

We apply Graf's addition theorem to the Bessel function $\mathrm{J}_0(kR)$ in Eq. (17). Following Tranter (1968) we write

$$\mathrm{J}_0(kR) = \sum_{q=0}^{\infty}\delta_q\mathrm{J}_q(kr)\mathrm{J}_q(k\rho)\cos\,q(\theta-\varphi), \tag{18}$$

where $\mathrm{J}_0(kR)$ is represented as a combination of the Bessel functions $\mathrm{J}_q(kr)$ and $\mathrm{J}_q(k\rho)$, $\delta_0 = 1$ and $\delta_q = 2$ for $q>0$. Finally, the Green's function in polar coordinates for deep water takes the form

$$\mathscr{G}(\rho,\varphi;r,\theta) = -2\int_0^{\infty}\frac{k}{k-k_0}\sum_{q=0}^{\infty}\delta_q\mathrm{J}_q(kr)\mathrm{J}_q(k\rho)\cos\,q(\theta-\varphi)\,\mathrm{d}k. \tag{19}$$

The Green's function for finite water-depth case obeys the conditions at the free surface, at the bottom $\mathscr{G}_z = 0$, and the radiation condition. The three-dimensional Green's function at $z=\zeta=0$ has the following form in polar coordinates:

$$\mathscr{G}(\rho,\varphi;r,\theta) = -2\int_{\mathscr{L}}\frac{k\cosh kh}{k\sinh kh - K\cosh kh}\,\mathrm{J}_0(kR)\,\mathrm{d}k, \tag{20}$$

where $\mathscr{L}$ is the contour of the integration in the complex k-plane, given in Fig. 2. Again we apply Graf's addition theorem to the Bessel function in the integrand, and the Green's function takes the form

$$\mathscr{G}(\rho,\varphi;r,\theta) = -2\int_0^{\infty}\frac{k\cosh kh}{k\sinh kh - K\cosh kh}\sum_{q=0}^{\infty}\delta_q\mathrm{J}_q(kr)\mathrm{J}_q(k\rho)\cos\,q(\theta-\varphi)\,\mathrm{d}k. \tag{21}$$

As in the eigenfunction approach [see, e.g., Kim and Ertekin (1998) for the finite depth case and Meylan and Squire (1996) for the infinite depth case], we represent the plate deflection as a series of Bessel functions with corresponding coefficients of the form

$$w(\rho,\varphi) = \sum_{m=1}^{M}\sum_{n=0}^{\infty}a_{mn}\mathrm{J}_n(\kappa_m\rho)\cos\,n\varphi, \tag{22}$$

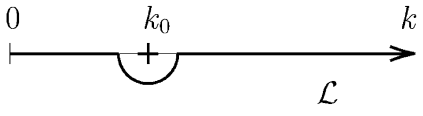

Fig. 2. Contour of the integration.

where a_{mn} are unknown amplitude functions and κ_m are the reduced wavenumbers. It will be shown later that κ_m, $m = 1, \ldots, M$, obeys the plate dispersion relation. M is the number of wave modes, i.e., number of roots of the plate dispersion relation, taken into account.

For numerical computations the upper limit of q in Eq. (19) or Eq. (21) and n in Eq. (22) will be taken as N, which is a truncation parameter of the problem. We can do this because of the decaying behavior of the Bessel functions with increasing order. Convergence of the final results is verified in the numerical computations. All terms of the order higher than N are negligibly small.

In the next section we apply the Green's theorem at $z = \zeta = 0$. Application of Green's theorem at $z<0$ together with expansion (22) gives rise to the standard eigenfunction expansion as can be found in Meylan and Squire (1996) for the potential.

4. Infinite water depth

Here we apply Green's theorem to obtain the integro-differential equation for the potential and vertical displacements. Then an approximate solution is derived for the more theoretical and less complicated case of deep water. The deep-water case is a good intermediate step for deriving the solution for the finite water-depth case, which is of our main interest. The main integro-differential equation has been derived for the general three-dimensional situation in Hermans (2001) and Andrianov and Hermans (2003). Now we rederive it in polar coordinates for the problem of the circle.

Application of Green's theorem leads to the following expression at $z = \zeta = 0$ for the total potential:

$$4\pi\phi(\rho,\varphi) = 4\pi\phi^{\mathrm{inc}}(\rho,\varphi) + \int_{\mathscr{P}} \left(K\phi(r,\theta) - \frac{\partial\phi(r,\theta)}{\partial\zeta} \right) \mathscr{G}(\rho,\varphi;r,\theta) r \,\mathrm{d}r \,\mathrm{d}\theta, \tag{23}$$

where the free-surface condition for the Green's function has been used.

We use the notation $\phi^{\mathscr{F}}$ for the potential function in open water region $\mathscr{F}$, it is the superposition of the incident wave potential ϕ^{inc} and ϕ^{dis}, which is the sum of the classical diffraction potential and radiation potential, as follows:

$$\phi^{\mathscr{F}} = \phi^{\mathrm{inc}} + \phi^{\mathrm{dis}}. \tag{24}$$

The potential ϕ^{dis} must satisfy the Sommerfeld radiation condition

$$\sqrt{\rho}\left(\frac{\partial}{\partial\rho} - \mathrm{i}k_0 \right) \phi^{\mathrm{dis}} = 0 \tag{25}$$

as $\rho \to \infty$. The total potential in the area covered by the plate $\mathscr{P}$ is denoted by $\phi^{\mathscr{P}}$.

Using the dynamic condition (9) for the plate region $\mathscr{P}$ to express $\phi^{\mathscr{P}}$ in terms of an operator acting on $\phi_z^{\mathscr{P}}$, we obtain the following equation:

$$\{\mathscr{D}\Delta^2 - \mu + 1\}\phi_z^{\mathscr{P}} = \frac{K}{4\pi} \int_{\mathscr{P}} \{\mathscr{D}\Delta^2 - \mu\}\phi_\zeta^{\mathscr{P}} \mathscr{G}(\rho,\varphi;r,\theta) r \,\mathrm{d}r \,\mathrm{d}\theta + \phi_z^{\mathrm{inc}}, \tag{26}$$

where for the last term, which represents the potential of the incoming waves, condition (10) has been used. Relation (26) is suitable for further analysis—to end up with the integro-differential equation for the plate deflection. We switch from the potential to the deflection function by use of the expression

$$\phi_z^{\mathscr{P}} = \frac{\omega}{\mathrm{i}} w, \tag{27}$$

derived from Eq. (2). Hence, the following equation is obtained:

$$\{\mathscr{D}\Delta^2 - \mu + 1\}w(\rho,\varphi) = \frac{K}{4\pi} \int_{\mathscr{P}} \{\mathscr{D}\Delta^2 - \mu\} w(r,\theta) \mathscr{G}(\rho,\varphi;r,\theta) r \,\mathrm{d}r \,\mathrm{d}\theta + A\mathrm{e}^{\mathrm{i}k_0\rho\cos\varphi} \tag{28}$$

for the plate deflection w at the free surface $z = 0$. Eq. (28) can be considered as the governing equation for the problem of the diffraction of surface waves on the circular plate, which floats in deep water.

We insert the relations for the deflection (22) and Green's function (19) into Eq. (28) and obtain the following integro-differential equation:

$$\{\mathscr{D}\Delta^2-\mu+1\}\sum_{m=1}^{M}\sum_{n=0}^{N}a_{mn}\,\mathrm{J}_n(\kappa_m\rho)\cos n\varphi + \frac{K}{2\pi}\int_0^{2\pi}\int_0^{r_0}\{\mathscr{D}\Delta^2-\mu\}\sum_{m=1}^{M}\sum_{n=0}^{N}a_{mn}\mathrm{J}_n(\kappa_m r)\cos n\theta \times\left(\int_0^{\infty}\frac{k}{k-k_0}\sum_{q=0}^{N}\delta_q\mathrm{J}_q(kr)\mathrm{J}_q(k\rho)\cos q(\theta-\varphi)\,\mathrm{d}k\right)r\,\mathrm{d}r\,\mathrm{d}\theta = A\sum_{n=0}^{N}\varepsilon_n\mathrm{J}_n(k_0\rho)\cos n\varphi, \tag{29}$$

where $\varepsilon_n=\delta_n\mathrm{i}^n$. Due to the orthogonality relation for the cosine functions we only get a nonzero contribution in the integrand for $n=q$. Next we work out the integration with respect to r and θ. The integration over r, in accordance with Korn and Korn (1968), gives us

$$\int_0^{r_0}\mathrm{J}_n(kr)\mathrm{J}_n(\kappa_m r)r\,\mathrm{d}r=\frac{r_0}{(k^2-\kappa_m^2)}\left[k\mathrm{J}_{n+1}(kr_0)\mathrm{J}_n(\kappa_m r_0)-\kappa_m\mathrm{J}_n(kr_0)\mathrm{J}_{n+1}(\kappa_m r_0)\right], \tag{30}$$

while the integration over θ gives us 2π for $n=0$ and $\delta_n\pi\cos n\varphi$ for $n>0$, and then $2\pi\cos n\varphi$ for all n.

In such a way, the following set of $N+1$ equations is obtained from the integro-differential equation (29):

$$\sum_{m=1}^{M}(\mathscr{D}\kappa_m^4-\mu+1)a_{mn}\mathrm{J}_n(\kappa_m\rho)+Kr_0\int_0^{\infty}\sum_{m=1}^{M}(\mathscr{D}\kappa_m^4-\mu)a_{mn}\mathrm{J}_n(k\rho) \times\frac{k}{(k-k_0)(k^2-\kappa_m^2)}\left[k\mathrm{J}_{n+1}(kr_0)\mathrm{J}_n(\kappa_m r_0)-\kappa_m\mathrm{J}_n(kr_0)\mathrm{J}_{n+1}(\kappa_m r_0)\right]\mathrm{d}k=A\varepsilon_n\mathrm{J}_n(k_0\rho), \tag{31}$$

where $n=0,\ldots,N$. Here $k=\kappa_m$ is not a singularity of the integrand. For plates with one infinite dimension, the deflection can be represented as a superposition of exponential functions. Therefore, it is easier to work out the integration over k in the integro-differential equation for those plates. For a circular plate, the integration in the complex plane needs special attention, as described below.

If we are at the plate region $\mathscr{P}$ ($\rho<r_0$), we represent the Bessel function $\mathrm{J}_q(kr_0)$, where q is n or $n+1$, as the half-sum of Hankel functions of the first and second kind

$$\mathrm{J}_q(kr_0)=\frac{\mathrm{H}_q^{(1)}(kr_0)+\mathrm{H}_q^{(2)}(kr_0)}{2}. \tag{32}$$

Then the integral in Eq. (31) is split up in two; these two we transform into integrals along the vertical axis in the complex k-plane plus the sum of the residues. All poles in the complex plane are shown in Fig. 3. For the first integral with $\mathrm{H}_q^{(1)}(kr_0)$, the contour can be closed in the upper half-plane with the poles $k=\kappa_m$, and for the second one with $\mathrm{H}_q^{(2)}(kr_0)$ in the lower half-plane, where the poles are $k=-\kappa_m$.

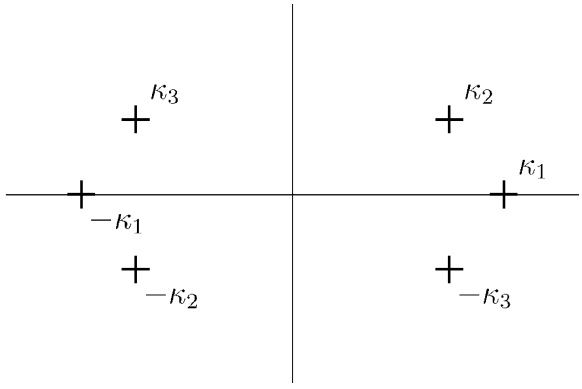

Fig. 3. Zeros of the dispersion relation for deep water.

We consider two situations separately to derive the plate dispersion relation. In the first integral each of the Bessel functions with the argument $\kappa_m r_0$ is represented as the half-sum of Hankel functions of first and second kind. After an application of Cauchy residue lemma to the integrand at the poles $k = \kappa_m$, the Wronskian W can be used, see, e.g., Abramowitz and Stegun (1964), in those poles for the combination of Hankel functions:

$$W\{\mathrm{H}_n^{(1)}(\kappa_m r_0), \mathrm{H}_n^{(2)}(\kappa_m r_0)\} = \mathrm{H}_{n+1}^{(1)}(\kappa_m r_0)\mathrm{H}_n^{(2)}(\kappa_m r_0) - \mathrm{H}_n^{(1)}(\kappa_m r_0)\mathrm{H}_{n+1}^{(2)}(\kappa_m r_0) = -\frac{4\mathrm{i}}{\pi\kappa_m r_0}. \tag{33}$$

For the second integral we apply the procedure described above and use the fact that $\mathrm{H}_q^{(2)}(-\kappa_m r_0) = -\mathrm{e}^{q\pi\mathrm{i}}\mathrm{H}_q^{(1)}(\kappa_m r_0)$. The coefficients of $\mathrm{J}_n(\kappa r_0)$ are considered to derive the dispersion relation for deep water

$$(\mathscr{D}\kappa^4 - \mu + 1)\kappa = \pm k_0, \tag{34}$$

where the plus sign on the right-hand side corresponds to the first situation, and the minus sign to the second. The roots of the plate dispersion relation (34) are shown in Fig. 3: two real roots $\pm\kappa_1$, and four complex roots $\pm\kappa_2$ and $\pm\kappa_3$, which are symmetrically placed with respect to both the real and imaginary axes. Due to the symmetry of the Bessel function, three roots of the plate dispersion relation (34) are taken into account: real positive κ_1, complex κ_2 and κ_3 with equal imaginary parts and equal but opposite-sign real parts. The real root κ_1 represents the main travelling wave mode, and the two complex roots represent damped waves.

In this way, for the case of infinite water depth we use three roots of the plate dispersion relation, as for the semi-infinite plate in Andrianov and Hermans (2003), and in the equations of this section the upper limit of the summation M is equal to 3. For the case of finite depth, more than three roots are taken into account.

In the first integral we also obtain a contribution of the pole $k = k_0$ of the integrand. This contribution has to cancel the term on the right-hand side of Eq. (31). Because we use the deep water case as the introduction to the finite water-depth case, we do not consider the contribution of the integral along the imaginary axis, and that makes our solution approximate. The application of the Jordan lemma and the contribution of the pole $k = k_0$ lead us to $N + 1$ relations:

$$\pi\mathrm{i}r_0 \sum_{m=1}^{M} \frac{k_0^2}{k_0^2 - \kappa_m^2}[k_0\mathrm{H}_{n+1}^{(1)}(k_0 r_0)\mathrm{J}_n(\kappa_m r_0) - \kappa_m \mathrm{H}_n^{(1)}(k_0 r_0)\mathrm{J}_{n+1}(\kappa_m r_0)] \times(\mathscr{D}\kappa_m^4 - \mu)a_{mn} = A\varepsilon_n. \tag{35}$$

The system for the determination of the unknown amplitudes a_{mn} can be completed by the free edge conditions. We obtain $N + 1$ equations from each of the free edge conditions (14) and (15) at $\rho = r_0$:

$$\sum_{m=1}^{M}\left[\mathrm{J}_n(\kappa_m r_0)\left(-\kappa_m^2 + \frac{(1-\nu)n(n-1)}{r_0^2}\right) + \mathrm{J}_{n+1}(\kappa_m r_0)\kappa_m \frac{(1-\nu)}{r_0}\right]a_{mn} = 0, \tag{36}$$

$$\sum_{m=1}^{M}\left[\mathrm{J}_n(\kappa_m r_0)\left(-\frac{n}{r_0}\kappa_m^2 + \frac{(1-\nu)n^2(1-n)}{r_0^3}\right) + \mathrm{J}_{n+1}(\kappa_m r_0)\left(\kappa_m^3 + \frac{(1-\nu)n^2}{r_0^2}\kappa_m\right)\right]a_{mn} = 0. \tag{37}$$

In such a way we derive the system of $3N + 3$ equations, Eqs. (35)–(37), for the determination of $3N + 3$ amplitudes a_{mn}. When the amplitudes are known, the plate deflection can be calculated by Eq. (22).

5. Finite water depth

Here we consider the general case when the plate floats on water of finite depth. The governing integro-differential equation can be derived analogously to the work presented in the previous section. It takes the form of Eq. (28), the same as in the deep water case, where we use the Green's function for the finite water-depth case, see Eq. (21).

Inserting the relations for the plate deflection (22) and Green's function (21) in Eq. (28), we obtain the following expanded integro-differential equation for the water of finite depth:

$$\{\mathscr{D}\Delta^2-\mu+1\}\sum_{m=1}^{M}\sum_{n=0}^{N}a_{mn}\mathrm{J}_n(\kappa_m\rho)\cos n\varphi$$
$$=\frac{K}{2\pi}\int_0^{2\pi}\int_0^{r_0}\{\mathscr{D}\Delta^2-\mu\}\sum_{m=1}^{M}\sum_{n=0}^{N}a_{mn}\mathrm{J}_n(\kappa_m r)\cos n\theta\left(\int_0^{\infty}\frac{k\cosh kh}{K\cosh kh-k\sinh kh}\right.$$
$$\left.\times\sum_{q=0}^{N}\delta_q\mathrm{J}_q(kr)\mathrm{J}_m(k\rho)\cos q(\theta-\varphi)\,\mathrm{d}k\right)r\,\mathrm{d}r\,\mathrm{d}\theta+A\sum_{n=0}^{N}\varepsilon_n\mathrm{J}_n(k_0\rho)\cos n\varphi \tag{38}$$

at the free surface $z=0$. The case $q=n$ has to be considered only, as was done for infinitely deep water. First we close the contour of the integration. Then the integration with respect to r and θ in Eq. (38) leads us to the set of $N+1$ equations

$$\sum_{m=1}^{M}(\mathscr{D}\kappa_m^4-\mu+1)a_{mn}\mathrm{J}_n(\kappa_m\rho)+Kr_0\int_{\mathscr{L}}\sum_{m=1}^{M}(\mathscr{D}\kappa_m^4-\mu)a_{mn}\mathrm{J}_n(k\rho)$$
$$\times\frac{k\cosh kh}{(K\cosh kh-k\sinh kh)(k^2-\kappa_m^2)}\left[k\mathrm{J}_{n+1}(kr_0)\mathrm{J}_n(\kappa_m r_0)-\kappa\mathrm{J}_n(kr_0)\mathrm{J}_{n+1}(\kappa_m r_0)\right]\mathrm{d}k$$
$$=A\varepsilon_n\mathrm{J}_n(k_0\rho), \tag{39}$$

where $n=0,\ldots,N$.

Now we consider the meromorphic function

$$p(k)=\frac{k\cosh kh}{K\cosh kh-k\sinh kh}. \tag{40}$$

The poles of function $p(k)$ are the roots of the dispersion relation for water region (12) $k=\pm k_i$, $i=0,\ldots,M-3$, where k_0 is the positive real root, and k_i, for $i\neq 0$, is the positive imaginary root, as shown in Fig. 4. The function $p(k)$ is bounded for all roots. Then the meromorphic function for our problem can be described by the following relation:

$$p(k)=\sum_{i=0}^{M-3}\frac{k_i^2}{k_i^2h-K^2h+K}\left(\frac{1}{k+k_i}+\frac{1}{k-k_i}\right). \tag{41}$$

This procedure has been applied in John (1950) and previously described by Whittaker and Watson (1920). The upper bound in the summation is chosen in accordance with the number of imaginary roots of the water dispersion relation (12).

Next, we insert relation (41) into Eq. (39), where we consider two integrals in the complex k-plane, which can be combined into one integral from $-\infty$ to $+\infty$ with the poles $k=k_i$ only. Finally, we derive the governing

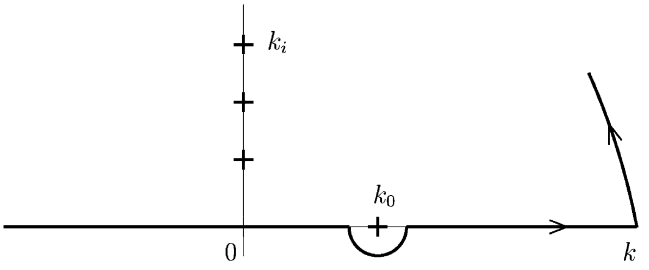

Fig. 4. Closure of the integration contour in the upper half-plane.

integro-differential equation for the case of finite water depth

$$\sum_{m=1}^{M}(\mathscr{D}\kappa_m^4-\mu+1)a_{mn}\mathrm{J}_n(\kappa_m\rho)+Kr_0\int_{-\infty}^{\infty}\sum_{m=1}^{M}(\mathscr{D}\kappa_m^4-\mu)a_{mn}\frac{\mathrm{J}_n(k\rho)}{(k^2-\kappa_m^2)}\times\sum_{i=0}^{M-3}\frac{k_i^2}{(k_i^2h-K^2h+K)(k-k_i)}[k\mathrm{J}_{n+1}(kr_0)\mathrm{J}_n(\kappa_m r_0)-\kappa_m\mathrm{J}_n(kr_0)\mathrm{J}_{n+1}(\kappa_m r_0)]\,\mathrm{d}k=A\varepsilon_n\mathrm{J}_n(k_0\rho) \tag{42}$$

at $z=0$. Now we have to work out the integration in the complex plane, that can be done analogously to the deep water case. The contour of the integration is depicted in Fig. 4.

We split up the Bessel functions with the argument kr_0 into half-sums of Hankel functions by Eq. (32) and then the integral in Eq. (42) becomes a sum of the integrals in the upper and lower half-planes. The sum of the residues gives us the same result in both situations due to the property of the meromorphic function. Also Wronskian (33) can be used for the combination of the Hankel functions. The residue lemma is applied at the poles $k=\kappa_m$, that leads to the standard dispersion relation for water of finite depth if we consider the coefficients of $\mathrm{J}_n(\kappa r_0)$. The plate dispersion relation has the following form:

$$(\mathscr{D}\kappa^4-\mu+1)\kappa\tanh\kappa h=K. \tag{43}$$

The dispersion relation (43) has two real roots $\pm\kappa_1$, and four complex roots $\pm\kappa_2$ and $\pm\kappa_3$, symmetrically placed with respect to both the real and imaginary axes, those six being of the same order as in the deep-water case, as well as infinitely many purely imaginary roots. Here we take into account M roots of Eq. (43): one real positive root κ_1, and two complex roots κ_2 and κ_3, with equal imaginary parts and equal but opposite-signed real parts, as well as $M-3$ imaginary roots, all located in the upper half-plane. We notice that the position of the roots κ_m in the complex k-plane is similar to the roots of the water dispersion relation (12), except of the two complex roots κ_2 and κ_3. The derivation of the dispersion relation (43) from IDE (42) is a good way to check the correctness of our approach.

Then we consider the contribution of the roots of the water dispersion relation, plotted in Fig. 4. The contour of integration for the integrals with $\mathrm{H}_q^{(1)}(kr_0)$ may be closed in the upper-half plane, and for the integrals with $\mathrm{H}_q^{(2)}(kr_0)$ in the lower half-plane. In the latter case we get a zero contribution because the poles are as indicated in the Fig. 4. The application of the Cauchy theorem to the integral closed in the upper half-plane gives the following $N+1$ equations to determine the amplitudes a_{mn}:

$$\pi\mathrm{i}Kr_0\sum_{m=1}^{M}\frac{k_0^2}{(k_0^2-\kappa_m^2)(k_0^2h-K^2h+K)}\times[k_0\mathrm{H}_{n+1}^{(1)}(k_0r_0)\mathrm{J}_n(\kappa_m r_0)-\kappa_m\mathrm{H}_n^{(1)}(k_0r_0)\mathrm{J}_{n+1}(\kappa_m r_0)](\mathscr{D}\kappa_m^4-\mu)a_{mn}=A\varepsilon_n, \tag{44}$$

and the poles at the imaginary axis $k=k_i$ result in a set of $(M-3)(N+1)$ equations:

$$\pi\mathrm{i}Kr_0\sum_{m=1}^{M}\frac{k_i^2}{(k_i^2-\kappa_m^2)(k_i^2h-K^2h+K)}\times[k_i\mathrm{H}_{n+1}^{(1)}(k_ir_0)\mathrm{J}_n(\kappa_m r_0)-\kappa_m\mathrm{H}_n^{(1)}(k_ir_0)\mathrm{J}_{n+1}(\kappa_m r_0)](\mathscr{D}\kappa_m^4-\mu)a_{mn}=0, \tag{45}$$

where $i=1,\ldots,M-3$. The edge conditions (36) and (37) give us $2(N+1)$ equations as in previous section. So, we derive the system of $M(N+1)$ equations, Eqs. (44), (45), (36), (37), to determine the amplitudes a_{mn} for the plate floating in water of finite depth. After solving of this system, the deflection of the circular plate can be computed by formula (22).

The finite depth model can be used for the problems of shallow water, and the results obtained are of higher accuracy, as more roots of the water and plate dispersion relations are taken into account.

6. Initiated wave pattern and free-surface elevation

Here we study the total free-surface elevation and a wave pattern, generated by the plate motion. It is possible to determine the free-surface elevation with the use of our approach for the plate-water interaction and integro-differential equation. The wave field initiated by the plate motion is the sum of the scattered and diffracted wave fields.

The total potential in $\mathscr{F}$ ($r > r_0$) is represented in Eq. (24) as the sum of the incident wave potential and the potential of waves which appeared due to the plate vibration. Therefore, the free-surface elevation ζ in the open fluid region $\mathscr{F}$ equals to the sum of the incident wave elevation and the additional wave elevation generated by the plate motion,

$$\zeta(\rho,\varphi) = \zeta^{\mathrm{inc}}(\rho,\varphi) + \zeta^{\mathrm{pm}}(\rho,\varphi), \tag{46}$$

where the value of elevation ζ^{inc} is known, as it is the parameter of the incident wave field, and the value of ζ^{pm} may be obtained from the analysis of an integro-differential equation.

Analogously to the treatment of the plate area $\mathscr{P}$ we can derive, for the region $\mathscr{F}$, from Eq. (26) the expression

$$\zeta = A\mathrm{e}^{\mathrm{i}k_0\rho\,\cos\,\varphi} + \frac{K}{4\pi}\int_{\mathscr{P}} \{\mathscr{D}\Delta^2 - \mu\} w(r,\theta)\mathscr{G}(\rho,\varphi;r,\theta) r\,\mathrm{d}r\,\mathrm{d}\theta. \tag{47}$$

Finally, with the use of Eq. (47), we obtain the following expression for the free-surface elevation for the water of infinite depth:

$$\zeta(\rho,\varphi) = A\mathrm{e}^{\mathrm{i}k_0\rho\,\cos\,\varphi} - \pi\mathrm{i}r_0 \sum_{m=1}^{M} \frac{k_0^2}{(k_0^2-\kappa_m^2)} (\mathscr{D}\kappa_m^4 - \mu) \times \sum_{n=0}^{N} a_{mn}[k_0 \mathrm{J}_{n+1}(k_0 r_0)\mathrm{J}_n(\kappa_m r_0) - \kappa_m \mathrm{J}_n(k_0 r_0)\mathrm{J}_{n+1}(\kappa_m r_0)]\mathrm{H}_n^{(1)}(k_0\rho)\,\mathrm{d}k. \tag{48}$$

To obtain this result previously the residue lemma at the pole $k = k_0$ is used.

For the case of finite water depth, after the use of the residue lemma at the poles $k = k_i$, we obtain the following expression for the free-surface elevation:

$$\zeta(\rho,\varphi) = A\mathrm{e}^{\mathrm{i}k_0\rho\,\cos\,\varphi} - \pi\mathrm{i}Kr_0 \sum_{m=1}^{M}\sum_{i=0}^{M-3} \frac{k_i^2}{(k_i^2-\kappa_m^2)(k_i^2 h - K^2 h + K)} (\mathscr{D}\kappa_m^4 - \mu) \times \sum_{n=0}^{N} a_{mn}[k_i \mathrm{J}_{n+1}(k_i r_0)\mathrm{J}_n(\kappa_m r_0) - \kappa_m \mathrm{J}_n(k_i r_0)\mathrm{J}_{n+1}(\kappa_m r_0)]\mathrm{H}_n^{(1)}(k_i\rho)\,\mathrm{d}k. \tag{49}$$

Expressions (48) and (49) are for the total free-surface elevation. To study the initiated wave pattern, i.e., to see the consequence of the plate presence, the incident field may be subtracted out from these expressions. The second terms on the right-hand sides of formulas (48) and (49) represent ζ^{pm} for the cases of infinite and finite water-depth, respectively. The details of numerical computation are given in the next section.

7. Numerical results and discussion

In this section, numerical results are given for the hydroelastic behavior of the circular plate for different values of the physical parameters. Results are presented for relevant and practically important cases. Also some remarks on the numerical calculation and notes about the results obtained are given.

The calculation of the Bessel functions of complex argument, including κ_2 and κ_3, has to be carried out carefully. The amplitudes a_{mn} of each wave mode behave as decaying functions because of the decay of the Bessel functions with respect to the order n, common for the Bessel functions and amplitudes. Similar behavior of these amplitudes was reported by Zilman and Miloh (2000) for shallow water. If we increase the value of flexural rigidity or radius, the decay is faster. Taking into account first the 30 terms of the series results in sufficient accuracy for realistic values of rigidity. Even for very low rigidity, taking of this number of the terms is sufficient too.

To avoid difficulties in the numerical computation when the argument of the function is small, in principle it is possible to use the recurrence relation described in Abramowitz and Stegun (1964),

$$\mathscr{C}_{n+1}(z) = \frac{2n}{z}\mathscr{C}_n(z) - \mathscr{C}_{n-1}(z), \tag{50}$$

where $\mathscr{C}$ denotes functions J, $\mathrm{H}^{(1)}$ or $\mathrm{H}^{(2)}$ in our formulation, and z denotes the arguments in the corresponding functions.

Numerical calculations are based on various values of the plate radius and flexural rigidity, while Poisson's ratio $\nu = 0.25$ and ratio $m/\rho_w = 0.25\,\mathrm{m}$ are constant. Taking the wave amplitude as $A = 1\,\mathrm{m}$, the water depth and incident wavelength are varied, which lead to different values of the wavenumber k_0 and of the frequency ω. The number of the Bessel function modes, which are taken into account, as described above, is $N = 30$. The number of the roots of the

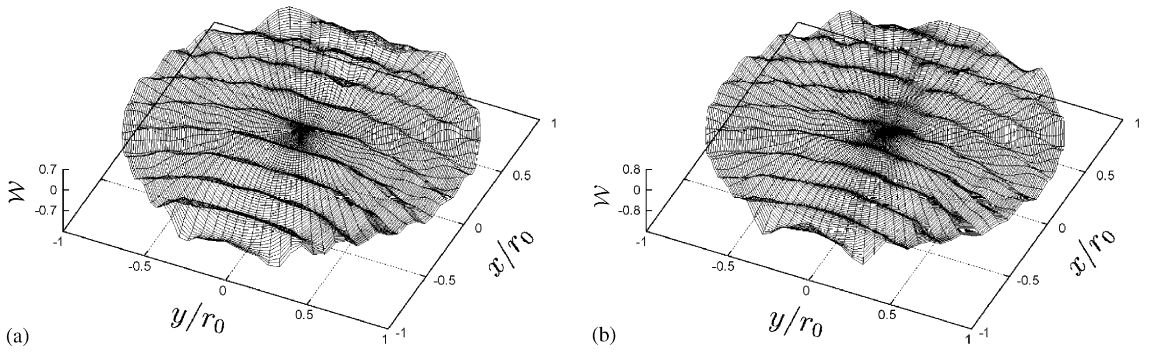

Fig. 5. Deflection of the circular plate, for $\lambda = 50\,\mathrm{m}$, $r_0 = 500\,\mathrm{m}$, $\mathscr{D} = 10^5\,\mathrm{m}^4$: (a) infinite depth, (b) finite depth, $h = 20\,\mathrm{m}$.

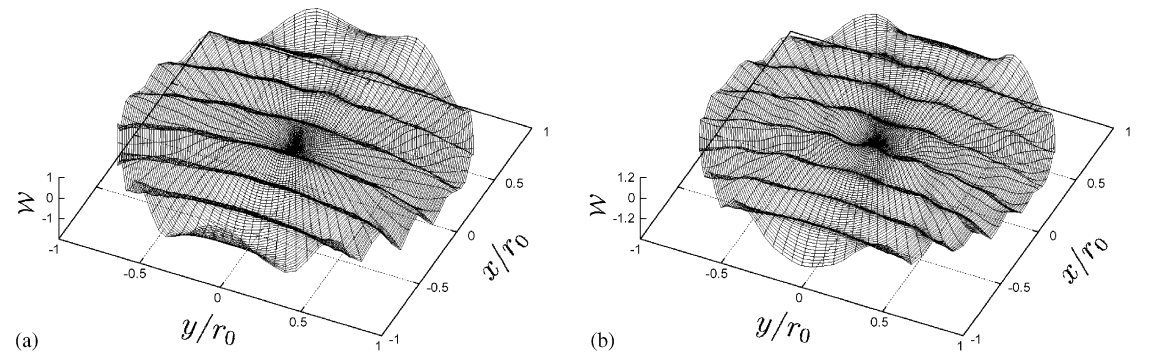

Fig. 6. Deflection of the circular plate, as in Fig. 5, for $\lambda = 100\,\mathrm{m}$.

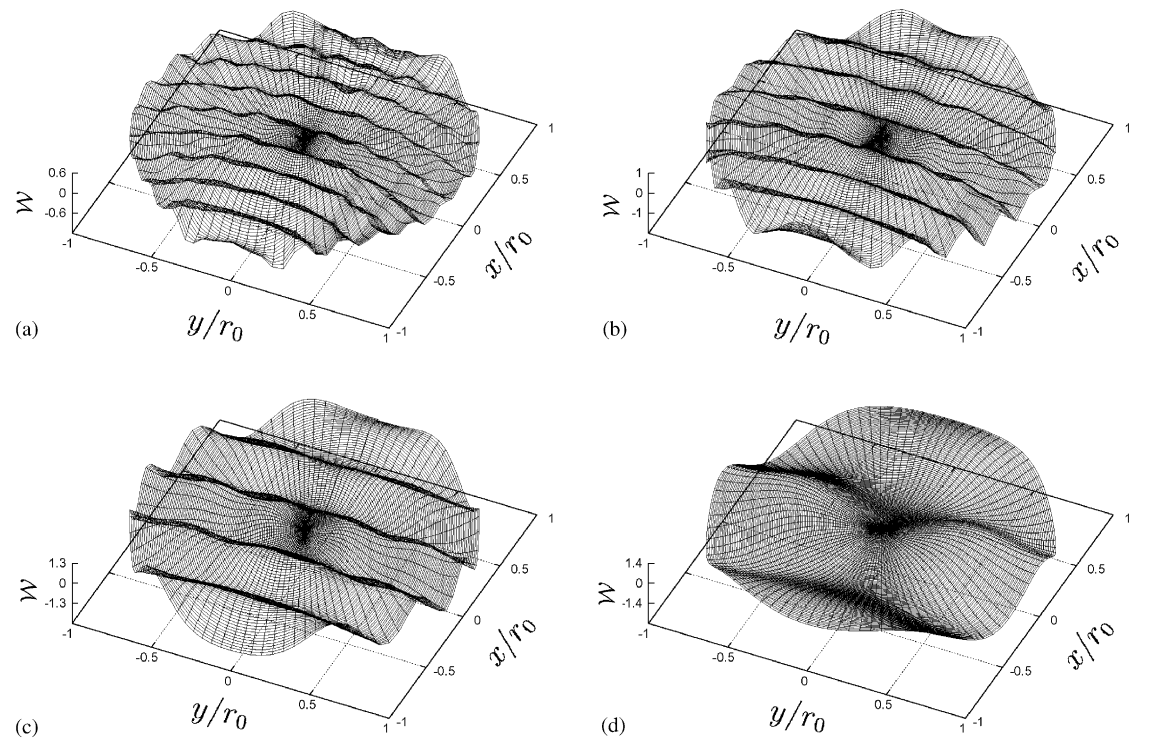

Fig. 7. Deflection of the circular plate, for $h = 100\,\mathrm{m}$, $r_0 = 500\,\mathrm{m}$, $\mathscr{D} = 10^5\,\mathrm{m}^4$: (a) $\lambda = 50\,\mathrm{m}$, (b) $\lambda = 100\,\mathrm{m}$, (c) $\lambda = 200\,\mathrm{m}$, (d) $\lambda = 500\,\mathrm{m}$.

plate dispersion relation for the finite water-depth case (43), which are taken into account, is $M = 10$. Especially for shallow water, the difference of the results due to the number of roots M can be hardly seen, while for the case of deep water the influence of the number of roots can be seen in the area close to the plate edge. The choice of such values of truncation parameters M and N was also justified by numerical tests. More details about the number of the roots has been published in Andrianov and Hermans (2003).

The numerical results are plotted for the real part of the plate deflection normalized by the wave amplitude $\mathrm{Re}(w)/A$, denoted by $\mathscr{W}$ in the figures. The results for both cases of the water depth are shown in the figures for a constant plate radius and rigidity and different wavelengths and water depths. The results for the circular plate on water of infinite depth are shown in Figs. 5(a) and 6(a). The results for the case of finite water depth are shown in all other subplots of Figs. 5–8. We can see clearly the wave propagation through the plate area.

The figures shown demonstrate that the wave travelling through the plate propagates with a curved wave front. This is especially prominent for cases when the wavelength is much smaller than the diameter of the circle. The plate deflection is highly dependent on the ratio between its radius r_0 and the wavelength λ. We found that for the rigidity $\mathscr{D} > 10^7\,\mathrm{m}^4$, the plate behaves as a very rigid body, whereas for $\mathscr{D} < 10^3\,\mathrm{m}^4$, the plate has hardly any influence on the surface waves. Realistic values of the reduced flexural rigidity $\mathscr{D}$ are of the order of about $10^7\,\mathrm{m}^4$ for the plate, while for ice it can be of the order of about $10^5\,\mathrm{m}^4$. The rigidity of the floating platform, Young's modulus and Poisson's ratio are highly dependent on the type of the structure and material used. In a zone close to the plate edge the deflection displays special behavior and can be quite different from the deflection in the center zone for low rigidity of the floating plate.

Also we found that computational results for large values of depth, $h > 100\,\mathrm{m}$, are almost independent of water depth. So, for such deep water, the depth does not have a strong influence on the results, and for this situation it is sufficient to take $M = 10$ as well. With decreasing water depth the results for the plate deflection and free-surface elevation are changing gradually, and then the water depth itself has a growing influence on the results.

For smaller values of the plate rigidity or stiffness the plate deflection increases. If the wavelength is decreasing, then the value of the deflection grows. The deflection is larger numerically also when the water depth increases.

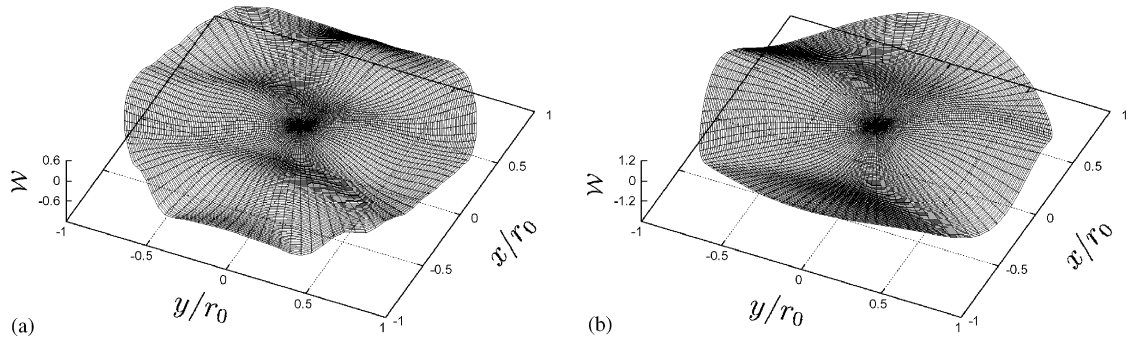

Fig. 8. Deflection of the circular plate, for $h = 100\,\mathrm{m}$, $r_0 = 500\,\mathrm{m}$, $\mathscr{D} = 10^7\,\mathrm{m}^4$: (a) $\lambda = 100\,\mathrm{m}$, (b) $\lambda = 500\,\mathrm{m}$.

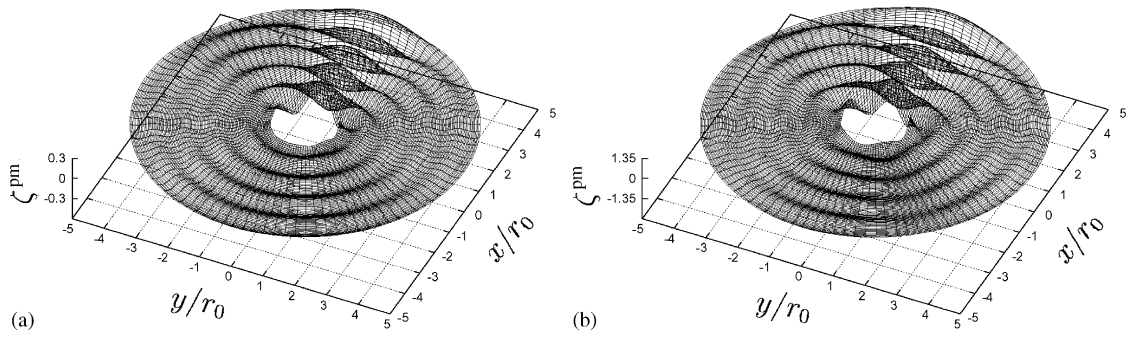

Fig. 9. Initiated wave pattern, for $h = 100\,\mathrm{m}$, $\lambda = 500\,\mathrm{m}$, $r_0 = 500\,\mathrm{m}$, $r_f = 2500\,\mathrm{m}$: (a) $\mathscr{D} = 10^6\,\mathrm{m}^4$, (b) $\mathscr{D} = 10^7\,\mathrm{m}^4$.

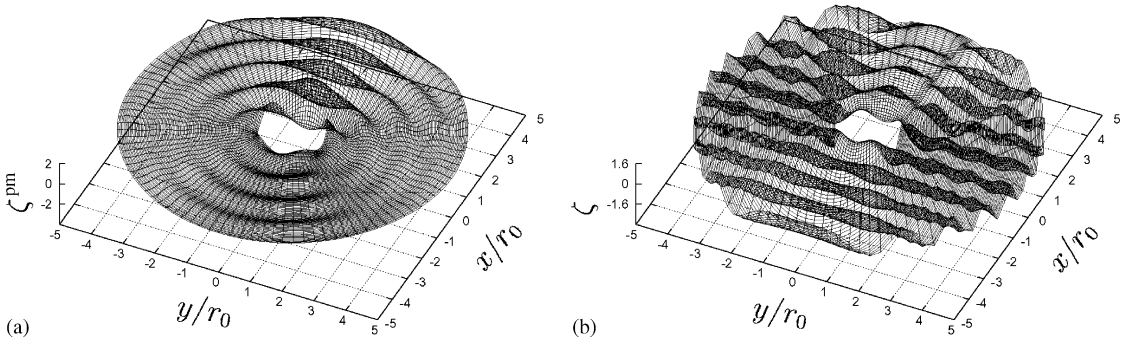

Fig. 10. (a) Initiated wave pattern and (b) free-surface elevation, for $\lambda = 500\,\mathrm{m}$, $r_0 = 500\,\mathrm{m}$, $r_f = 2500\,\mathrm{m}$, $\mathscr{D} = 10^8\,\mathrm{m}^4$.

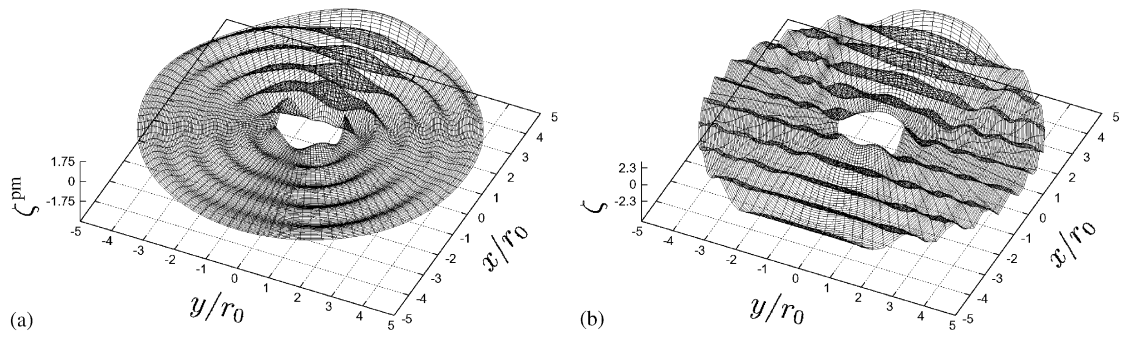

Fig. 11. (a) Initiated wave pattern and (b) free-surface elevation, for $h = 100\,\mathrm{m}$, $\lambda = 500\,\mathrm{m}$, $r_0 = 500\,\mathrm{m}$, $r_f = 2500\,\mathrm{m}$, $\mathscr{D} = 10^8\,\mathrm{m}^4$.

In Fig. 9 we show results for the initiated wave pattern, i.e. for the free-surface elevation ζ^{pm}, generated by the motion of the circular plate. The subplots are given for the surface of the fluid domain of radius r_f, for the water of finite depth. The initiated wave pattern is highly dependent on the water depth h and physical plate properties.

In Figs. 10 and 11 numerical results are given for the initiated wave pattern, subplots (a), and the free-surface elevation, subplots (b), for the cases of infinite and finite water depth. With the growth of the plate flexural rigidity (also stiffness or Poisson's ratio) the influence of the plate motion on the total elevation of the water surface grows as well. All figures are symmetric about the x-axis, because incoming plane waves propagate in the x-direction and their crests are parallel to the y-axis.

8. Conclusions and summary

The problem of the interaction between a floating elastic circular plate and incident surface waves is solved. The analytical and numerical study of the plate hydroelastic behavior is presented. The integro-differential equation for the problem is derived, and the algorithm of its numerical solution is proposed. For the case of finite water depth the system of equations for the expansion coefficients is obtained analytically. For infinitely deep water the problem is solved partly.

The finite water-depth model can be used to solve the plate–water interaction problem for the case of shallow or infinite depth. Taking the limits $h \to \infty$ and $h \to 0$, we can derive the dispersion relation relations for deep or shallow water from the dispersion for the water of finite depth. The floating platforms are located in offshore zones, usually close to shore. Normally, the water depth is rather small in such zones, but as the wavelength could be short and long it is more universal to use the finite water depth results to describe the response of the plates to ocean or sea waves.

The initiated wave pattern and the free-surface elevation in the open water region, the reflection and the transmission of incoming waves can also be described by the use of the derived integro-differential equation. In contrast to other papers, by means of our approach we may find the plate deflection and free-surface elevation using one set of the equations. The approach presented can be extended to other rotational symmetric configurations of the plate.

The approach is valid when the plate thickness and draft are assumed to be zero. To extend our method to the case of finite thickness of the plate, we may do the following. The deflection of the plate may be represented in the form

$$w = w^{(0)}(\kappa_m^{(0)}) + dw^{(1)}(\kappa_m^{(0)}, \kappa_m^{(1)}), \tag{51}$$

where $w^{(0)}$ is the solution obtained in the foregoing with the zero-thickness assumption, and $\kappa_m^{(0)}$ are the roots of the plate dispersion relation, also given in the foregoing, d is the draft of the plate, the superscripts denote the draft order. To avoid secular terms in $w^{(1)}$, $\kappa_m^{(0)}$ will be determined. The term $w^{(1)}$ then can be derived with use of the function $w^{(0)}$ and the extended dispersion relation for the first draft order, where the roots $\kappa_m^{(1)}$ are expressed via $\kappa_m^{(0)}$.

One of possible applications of the method is its use for the hydroelastic analysis of a VLFP for, say, a floating airport. The planform of a VLFP depends on the currents of the sea or ocean, where it is planned to place the floating airport, the distance from the coast, water depth, expected diffracted pattern, etc. In some cases it can make sense to construct the VLFP of an arbitrary horizontal shape, for instance, of a circular planform.

By inserting the physical properties of ice instead of those of the elastic plate, we can use the present approach to study the motion of large ice fields in water waves. There are so-called pancake ice fields with horizontal shape very close to a circle; in that case the ice-water interaction may be studied by the given theory.

References

Abramowitz, M., Stegun, I.A., 1964. Handbook of Mathematical Functions with Formulas, Graphs, and Mathematical Tables. U.S. Government Printing Office, Washington.

Andrianov, A.I., Hermans, A.J., 2003. The influence of water depth on the hydroelastic response of a very large floating platform. Marine Structures 16, 355–371.

Andrianov, A.I., Hermans, A.J., 2004. Hydroelasticity of elastic circular plate. Proceedings of 19th International Workshop on Water Waves and Floating Bodies, Cortona, Italy, pp. 7–10.

Hermans, A.J., 2001. A geometrical-optics approach for the deflection of a floating flexible platform. Applied Ocean Research 23, 269–276.

Hermans, A.J., 2003. The ray method for the deflection of a floating flexible platform in short waves. Journal of Fluids and Structures 17, 593–602.

John, F., 1950. On the motion of floating bodies, II. Communications on Pure and Applied Mathematics 3, 45–101.

Kim, J.W., Ertekin, R.C., 1998. An eigenfunction-expansion method for predicting hydroelastic behavior of a shallow-draft VLFS. Proceedings of second International Conference on Hydroelasticity in Marine Technology, Fukuoka, Japan, pp. 47–59.

Korn, G.A., Korn, T.M., 1968. Mathematical Handbook for Scientists and Engineers: Definitions, Theorems and Formulas for Reference and Review. McGraw-Hill, New York.

Meylan, M.H., 2001. A variation equation for the wave forcing of floating thin plates. Applied Ocean Research 23, 195–206.

Meylan, M.H., Squire, V.A., 1996. Response of a circular ice floe to ocean waves. Journal of Geophysical Research 101 (C4), 8869–8884.

Ohkusu, M., Namba Y., 1996. Analysis of hydroelastic behaviour of a large floating platform of thin plate configuration in waves. Proceedings of the International Workshop on Very Large Floating Structures, Hayama, Japan, pp. 143–148.

Peter, M.A., Meylan, M.H., Chung, H., 2003. Wave scattering by a circular plate in water of finite depth: a closed form solution. Proceedings of 13th International Offshore and Polar Engineering Conference, vol.1, Honolulu, USA, pp. 180–185.

Sturova, I.V., 2003. Response of unsteady external load on the elastic circular plate floating on shallow water. Proceedings of the 18th International Workshop on Water Waves and Floating Bodies, Le Croisic, France, pp. 177–180.

Takagi, K., 2002. Hydroelastic response of a very large floating structure in waves—a simple representation by the parabolic approximation. Applied Ocean Research 24, 175–183.

Timoshenko, S.P., Young, D.H., Weaver, W., 1974. Vibration Problems in Engineering. Wiley, New York.

Tranter, C.J., 1968. Bessel Functions with Some Physical Applications. The English Universities Press, London.

Tsubogo, T., 2001. The Motion of an elastic disk on shallow water in waves. Proceedings of 11th International Offshore and Polar Engineering Conference, vol.1, Stavanger, Norway, pp. 229–233.

Watanabe, E., Utsunomiya, T., Wang, C.M., Xiang, Y., 2003. Hydroelastic analysis of pontoon-type circular VLFS. Proceedings of 13th International Offshore and Polar Engineering Conference, vol.1, Honolulu, USA, pp. 93–99.

Watanabe, E., Utsunomiya, T., Wang, C.M., 2004. Hydroelastic analysis of pontoon-type VLFS: a literature survey. Engineering Structures 26, 245–256.

Wehausen, J.V., Laitone, E.V., 1960. Surface Waves. Encyclopedia of Physics, vol. 9. Springer, Berlin, 9, pp. 446–814 (also at http://www.coe.berkeley.edu/SurfaceWaves).

Whittaker, E.T., Watson, G.N., 1920. A Course of Modern Analysis. Cambridge University Press, Cambridge.

Zilman, G., Miloh, T., 2000. Hydroelastic buoyant circular plate in shallow water: a closed form solution. Applied Ocean Research 22, 191–198.